Explaining the GeV Antiproton Excess, GeV γ-Ray Excess, and W-Boson Mass Anomaly in an Inert Two Higgs Doublet Model

Cheng-Rui Zhu,[1,2] Ming-Yang Cui,[1,*] Zi-Qing Xia,[1] Zhao-Huan Yu,[3] Xiaoyuan Huang,[1,4,†]
Qiang Yuan,[1,4,‡] and Yi-Zhong Fan[1,4,§]
[1]*Key Laboratory of Dark Matter and Space Astronomy, Purple Mountain Observatory,*
Chinese Academy of Sciences, Nanjing 210023, China
[2]*Shandong Institute of Advanced Technology, Jinan 250100, China*
[3]*School of Physics, Sun Yat-Sen University, Guangzhou 510275, China*
[4]*School of Astronomy and Space Science, University of Science and Technology of China,*
Hefei 230026, Anhui, China

(Received 15 April 2022; revised 20 September 2022; accepted 31 October 2022; published 2 December 2022)

For the newly discovered W-boson mass anomaly, one of the simplest dark matter (DM) models that can account for the anomaly without violating other astrophysical and experimental constraints is the inert two Higgs doublet model, in which the DM mass (m_S) is found to be within ~54–74 GeV. In this model, the annihilation of DM via $SS \to b\bar{b}$ and $SS \to WW^*$ would produce antiprotons and gamma rays, and may account for the excesses identified previously in both particles. Motivated by this, we reanalyze the AMS-02 antiproton and Fermi-LAT Galactic center γ-ray data. For the antiproton analysis, the novel treatment is the inclusion of the charge-sign-dependent three-dimensional solar modulation model as constrained by the time-dependent proton data. We find that the excess of antiprotons is more distinct than previous results based on the force-field solar modulation model. The interpretation of this excess as the annihilation of $SS \to WW^*$ ($SS \to b\bar{b}$) requires a DM mass of ~40–80 (40–60) GeV and a velocity-averaged cross section of $O(10^{-26})\ \mathrm{cm}^3\,\mathrm{s}^{-1}$. As for the γ-ray data analysis, besides adopting the widely used spatial template fitting, we employ an orthogonal approach with a data-driven spectral template analysis. The fitting to the GeV γ-ray excess yields DM model parameters overlapped with those to fit the antiproton excess via the WW^* channel. The consistency of the DM particle properties required to account for the W-boson mass anomaly, the GeV antiproton excess, and the GeV γ-ray excess suggests a common origin of them.

DOI: 10.1103/PhysRevLett.129.231101

Introduction.—The dark matter (DM) problem remains one of the biggest mysteries of the cosmos. Among many kinds of candidates, the weakly interacting massive particle (WIMP) is the most naturally motivated by the thermal production in the early Universe and its proper relic density today [1]. Quite a lot of efforts have been spent in looking for WIMP DM in various kinds of experiments. No convincing signal has been identified in the direct detection experiments, and very stringent constraints on the WIMP-nucleon interaction strength have been set (e.g., Refs. [2,3]). As for the indirect detection aiming to identify the products of the annihilation or decay of the DM particles [1,4], some anomalies have been claimed in the past decade, such as the positron and electron excesses [5–7], the antiproton excess (See also Refs. [8,9] for possible hints of excess from measurements prior to AMS-02.) [10,11], and the Galactic center γ-ray excess (GCE) [12–15]. While the positron and electron excesses might be naturally explained by astrophysical pulsars [16,17] and the DM interpretation is severely constrained by γ-ray and cosmic microwave background observations [18], the antiproton excess and the GCE which point to a consistent DM interpretation survive other constraints [19–21]. Although uncertainties of various astrophysical and particle physics ingredients exist [22–32], common implications on the DM scenario from multimessengers are very interesting. In any case, additional tests of this scenario from independent probes are very important in finally detecting DM particles.

Very recently, the measured W-boson mass by the CDF collaboration showed ~7σ deviation from the prediction of the standard model (SM), which strongly suggests the existence of new physics beyond the SM [33]. One of the most economic solutions is to introduce an additional scalar doublet, in which the non-SM scalars can enhance the W-boson mass via the loop corrections. With a proper discrete symmetry $\mathbb{Z}_2$, the lightest new scalar in the doublet can be stable and play the role of DM. One realization of this mechanism is the inert two Higgs doublet model (i2HDM), which is shown to be able to accommodate the new W-boson mass and various astrophysical and experimental constraints simultaneously [34]. Considering available constraints from the collider searches for new physics, the electroweak precision tests, the direct detection of DM, and the relic density of DM, the mass of DM is limited within the range of 54 GeV $< m_S <$ 74 GeV, and the annihilation is dominated by the process of $SS \to WW^*$ for $m_S \geq 62$ GeV and by $SS \to b\bar{b}$ otherwise.

It is thus essential to examine whether the astrophysical data are in support of such an attractive possibility or not. For such a purpose, we reanalyze the AMS-02 antiproton and Fermi-LAT Galactic center γ-ray data. Compared with previous works, we improve the technical treatments in several aspects to reduce potential uncertainties of the analyses. For the antiproton modeling, our novel treatment is to include the charge-sign-dependent three-dimensional (3D) solar modulation model [35,36] as constrained by the time-dependent AMS-02 proton data [37]. To investigate the GCE, taking a data-driven method, we identify the background components for the γ-ray sky solely with their spectral properties as in Ref. [38], called the spectral template analysis. The traditional spatial template analysis will also be employed for a cross check. To minimize the possible contamination from the astrophysical contribution in the galactic bulge [28,29], a large portion of the galactic disk is masked. We find consistent DM particle properties to account for the W-boson mass anomaly, the GCE, and the antiproton excess, which are in favor of a common origin.

Antiprotons.—In previous studies, the solar modulation of the antiprotons is usually assumed to be the same as that of protons, and the force-field approximation [39] was often adopted (An empirical approach to derive a time, rigidity, and charge-sign dependent force-field modulation potential has been developed in Ref. [40].). However, it is known that the particles with opposite charge have very different trajectories in the heliosphere (e.g., Ref. [41]). Such an effect should be taken into account to properly reproduce the local interstellar spectra (LIS) of protons and antiprotons. For such a purpose, here we employ the charge-sign-dependent 3D solar modulation model developed in Refs. [42,43]. The transportation of charged particles inside the heliosphere is described by the Parker's equation [44]

$$\frac{\partial f}{\partial t} = -(\boldsymbol{V}_{\mathbf{sw}} + \langle \boldsymbol{v}_d \rangle) \cdot \nabla f + \nabla \cdot (\boldsymbol{K}^{(s)} \cdot \nabla f) + \frac{1}{3}(\nabla \cdot \boldsymbol{V}_{\mathbf{sw}}) \frac{\partial f}{\partial \ln p}, \qquad (1)$$

where $f(\boldsymbol{r}, p, t)$ is the phase space distribution function of cosmic rays, $\boldsymbol{V}_{\mathbf{sw}}$ is the solar wind speed, $\langle \boldsymbol{v}_d \rangle$ is the pitch-angle-averaged drift velocity, $\boldsymbol{K}^{(s)}$ is the symmetric diffusion tensor, and p is the momentum of the particle. See the Supplemental Material, Sec. A [45], for more details about the setup of the 3D modulation model, which includes Refs. [46–51]. We solve the Parker's equation numerically employing the stochastic differential equations [42,43].

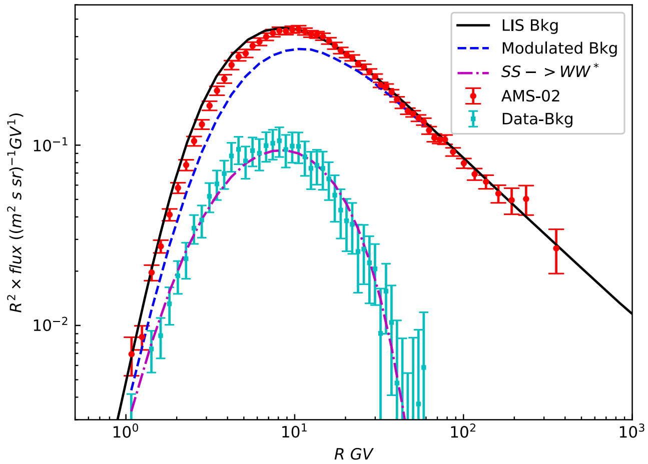

FIG. 1. The LIS (solid) and the modulated (dashed) spectra of background antiprotons, compared with the data [60]. The cyan points denote the AMS-02 data minus the modulated background results, and the dash-dotted line shows the antiproton spectrum from DM annihilation into WW^* with $(m_S, \langle \sigma v \rangle) = (62.6\ \text{GeV}, 1.5 \times 10^{-26}\ \text{cm}^3\ \text{s}^{-1})$.

The LIS of protons is derived through fitting to the Voyager-1 [52], AMS-02 [6], and DAMPE [53] data. To do this fitting, we employ the GALPROP [54] code to calculate the propagation of cosmic rays in the Milky Way [54]. The detailed fitting procedure is described in the Supplemental Material, Sec. B [45], which includes Refs. [55–57]. The antiproton LIS, calculated based on the proton LIS, is shown by the black solid line in Fig. 1. Here we use the new parameterization of the antiproton production cross section from Ref. [58] and an energy-dependent nuclear enhancement factor to take into account the contribution from heavy nuclei in both cosmic rays and the interstellar medium [59].

We fit the time-dependent proton fluxes measured by AMS-02 [37] to obtain the solar modulation parameters. The AMS-02 monthly proton fluxes are grouped into nine time bins; each contains six Bartels rotations, from May 19, 2011 to May 26, 2015, corresponding to the antiproton measurement time [60]. The fitting results of the main modulation parameters are given in the Supplemental Material, Sec. C [45], which includes Refs. [61–63]. Using the best-fit parameters, we calculate the modulated antiproton spectrum, as shown by the blue dashed line in Fig. 1. We find that the modulated background spectrum from the cosmic ray interactions is lower than the data between 1 and 30 GeV, consistent with previous studies [10,11,19]. Intriguingly, the difference between the antiproton data and the predicted astrophysical background is more distinct than that found previously with the force-field solar modulation. This is perhaps because particles with negative charge were modulated more severely than positive charged particles after the reversal of the heliospheric magnetic field [64].

Then we consider the DM contribution to the antiprotons. The DM density distribution is assumed to be a generalized Navarro-Frenk-White profile [65], with a local density of 0.4 GeV cm^{-3} and an inner slope of 1.28 (This density profile is consistent with the prediction from the cold DM model, which is largely consistent with observations of DM dominated systems, such as ultrafaint dwarf galaxies [66,67].). The annihilation into $b\bar{b}$ or W^+W^- is considered. For DM mass $m_S < m_W$, we also consider the off shell annihilation into WW^*, as in the case of i2HDM. The DM annihilation into WW^* is simulated with MadGraph5_aMC@NLO [68], including all three-body final states of one on-shell and one off-shell W boson. We further utilize PYTHIA 8 [69] to carry out the simulation of final state radiation, hadronization, and particle decays, and obtain the corresponding energy spectra of antiprotons and γ rays.

We perform a likelihood fitting to the antiproton data, with a marginalization of the constant rescaling factor of the background, and obtain the constraints on the $(m_S, \langle\sigma v\rangle)$ parameters. The results are shown in Fig. 2 for the WW^* channel, and the results for the $b\bar{b}$ channel are shown in the Supplemental Material, Sec. G [45]. The favored mass of DM particles is from 40 to 60 GeV for the $b\bar{b}$ channel, and from 40 to 80 GeV for the WW^* channel, respectively, and the annihilation cross section is around the level of the thermal production of DM, i.e., $\mathcal{O}(10^{-26}\ \mathrm{cm}^3\ \mathrm{s}^{-1})$. We also consider the influence of uncertainties of solar modulation on the likelihood fitting. The result is shown in the Supplemental Material, Sec. D [45]. We can see that the contours of WW^* overlap well with the i2HDM model parameters to fit the m_W anomaly [34]. Two possible regions of the i2HDM parameter space with DM mass of about 70–73 GeV (for four-point interactions) and about 62–63 GeV (for the Higgs resonance and scalar-pseudoscalar coannihilation region) can commonly account for the antiproton excess and the m_W anomaly. In the even lower-mass window ($m_S < 62$ GeV), the i2HDM model to fit the m_W anomaly typically requires DM to annihilate dominantly into $b\bar{b}$ but with a much smaller cross section and seems not able to produce enough antiprotons.

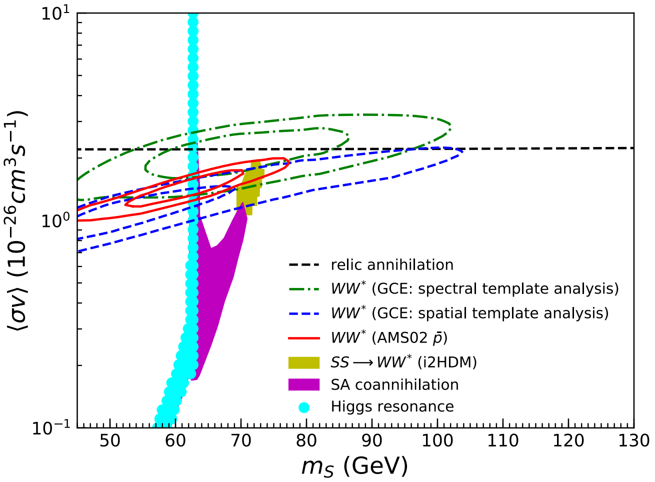

FIG. 2. The favored DM parameter space via fitting to the antiproton and GCE data (1σ and 2σ from inside to outside) for the WW^* channel, as well as the i2HDM model parameters to fit the W-boson mass anomaly (the 95% region, adopted from Ref. [34]). The black dashed line is the mass-dependent relic annihilation cross section [70].

Galactic center gamma rays.—The Galactic center is expected to gather high densities of DM, which makes it appealing for the indirect detection of DM. A spatially extended excess of γ rays in the 1–10 GeV energy range, with respect to the expected emission of cataloged point sources and astrophysical diffuse components, was found in the Fermi-LAT observations (e.g., Refs. [12–15]), named as the GCE.

To investigate this GeV excess, Refs. [38,71–73] adopt the spectral template analysis, which attempts to reduce the influences from uncertainty in spatial templates of astrophysical diffuse components. The γ-ray sky is decomposed into point sources and a diffuse emission component by $\mathrm{D}^3\mathrm{PO}$ and spectra from the “cloudlike” component and the “bubblelike” component, for diffuse emission from hadronic and leptonic processes were derived from two distinctive regions [71]. The astrophysical background is investigated by including point sources and data-driven spectral templates. Further, the spectral information of DM annihilation is used as a new component. The existence of the GCE was confirmed, and consistent DM parameters were derived in this alternative way if the spatial distribution of the GCE is fixed as in Ref. [15], although an indication of a spatial correlation between the GCE and astrophysical component was shown if the spatial distribution of the GCE is free [38]. Note that following Ref. [38], we also consider the isotropic component in the spectral template analysis. Though this component is subdominant in the Galactic center region, it would be important in the region far away from the Galactic disk. See more details of the spectral template analysis in Ref. [38].

Besides the annihilation channel of $SS \to b\bar{b}$ [38], here we apply this method to investigate whether the annihilation of DM via $SS \to WW^*$ could be consistent with the Galactic center γ-ray data. The γ-ray dataset, the point sources, and the spectra from the “cloudlike” component, the “bubblelike” component, and the isotropic γ-ray component are the same as in Ref. [38]. Here the DM density distribution is the same as that for the antiproton analysis in Sec. II. The region of interest (ROI) used in this analysis is a square region selected by Galactic latitudes $|b| < 20°$ and Galactic longitudes $|l| < 20°$, with a mask of the Galactic plane with $|b| < 8°$, to eliminate the influence from the boxy bulge, the nuclear bulge, and the X-shaped bulge [28,29].

We scan the DM parameters to calculate the likelihood map of different parameters. See Sec. E of the Supplemental Material [45] for the selected ROI and likelihood map of the GCE fitting. The best fit DM parameters we got are $(m_S, \langle\sigma v\rangle) = (68.5\ \mathrm{GeV}, 2.1 \times 10^{-26}\ \mathrm{cm}^3\,\mathrm{s}^{-1})$ for the WW^* channel, and (77.5 GeV, $1.7 \times 10^{-26}\ \mathrm{cm}^3\,\mathrm{s}^{-1}$) for the $b\bar{b}$ channel. The 1σ and 2σ contours of the fittings (WW^*) are given in Fig. 2 by green dash-dotted lines. At the 2σ level, the favored region of the WW^* channel from the GCE, the antiproton excess, and the m_W anomaly overlap with each other. Given that there should be additional uncertainties from various aspects of the theoretical modeling (e.g., the density profile of DM in the inner Galaxy and the simulation of the spectra of the annihilation final state particles), we regard these three anomalies as accounted for simultaneously with the same DM model component. The results for the $b\bar{b}$ channel are shown in the the Supplemental Material Sec. F.

As a complementary check, we also take the traditional spatial template regression techniques [13,15,32] to fit the Fermi-LAT γ-ray observations to investigate the GCE. See the Supplemental Material Sec. F [45] for more details of the spatial template analysis, which includes Refs. [74–78]. Corresponding to the minimums of mean χ^2 values, the best fit DM parameters $(m_S, \langle\sigma v\rangle)$ we obtained are (49.7 GeV, $1.0 \times 10^{-26}\ \mathrm{cm}^3\,\mathrm{s}^{-1}$) for the WW^* channel and (50.1 GeV, $6.7 \times 10^{-27}\ \mathrm{cm}^3\,\mathrm{s}^{-1}$) for the $b\bar{b}$ channel, respectively. The 1σ and 2σ contours (WW^*) for this spatial template analysis are shown in Fig. 2 as blue dashed lines. Similar to the result of the previous spectral template analysis, we also find the 2σ confidence region of the WW^* channel from the GCE, the antiproton excess, and the m_W anomaly invariably overlap with each other.

Conclusion and discussion.—Very recently, the CDF collaboration reported a statistically significant W-boson mass excess [33], which strongly indicates the new physics beyond the SM [79,80]. One interesting possible solution is the i2HDM, which indicates dark matter particles with a mass of ~50–70 GeV, and with the cross section $\sim\mathcal{O}(10^{-26}\ \mathrm{cm}^3\,\mathrm{s}^{-1})$ for the $SS \to WW^*$ annihilation channel. If correct it might yield observable gamma rays and antiprotons in the Galaxy. Motivated by such a possibility, in this Letter we reanalyze the Fermi-LAT γ-ray and AMS-02 antiproton data and then investigate the possible DM origin of the identified excesses. While our excess signals are generally in agreement with previous works, we incorporate several new technical treatments in the analysis such as the charge-sign-dependent 3D solar modulation of antiprotons and a spectral template fitting scheme of γ rays, as well as the off-shell annihilation channel of $SS \to WW^*$. It is very intriguing to find that the three very different anomalies can be simultaneously accounted for in a minimal DM model with DM particle mass of ~60–70 GeV. The velocity-weighted annihilation cross section is about $\langle\sigma v\rangle \sim O(10^{-26}\ \mathrm{cm}^3\,\mathrm{s}^{-1})$ and is just consistent with the expectation of the thermal production of DM. The required DM parameters are also consistent with constraints from other probes such as neutrinos [81]. Although there are various kinds of uncertainties of the antiproton background calculation like the propagation model of cosmic rays, the hadronic interaction models, and/or the solar modulation which is partially addressed in this Letter [22–25], as well as debates of the astrophysical or DM origin of the GCE [26–32], the DM interpretation of the three independent signals seems to be a straightforward, economic, and attractive possibility. The ongoing direct detection experiments such as the PandaX-4T, Xenon-nT, and LUX has a good prospect to detect it in the near future, as shown in Ref. [34].

We comment that the antiproton excess identified in 1–40 GeV (Fig. 1) is likely hard to be accounted for by astrophysical sources. As a commonly proposed scenario that secondary particles may also be produced via interactions around the accelerating sources (e.g., supernova explosion in molecular clouds), harder spectra of secondary particles are expected which should be more evident at high energies [82,83]. If we artificially attribute the identified low-energy antiproton excess to an astrophysical secondary particle component, the corresponding B/C ratio would be significantly higher than the measurements, as shown in the Supplemental Material of Ref. [10].

This work is supported by the National Key R&D program of China (No. 2021YFA0718404), the National Natural Science Foundation of China (No. 11921003, No. 11903084, No. 12003069, No. 12220101003), Chinese Academy of Sciences (CAS), the CAS Project for Young Scientists in Basic Research (No. YSBR-061), and the Program for Innovative Talents and Entrepreneurs in Jiangsu.

---

[*] Corresponding author.
mycui@pmo.ac.cn

[†] Corresponding author.
xyhuang@pmo.ac.cn

[‡] Corresponding author.
yuanq@pmo.ac.cn

[§] Corresponding author.
yzfan@pmo.ac.cn

[1] G. Bertone, D. Hooper, and J. Silk, Phys. Rep. **405**, 279 (2005).
[2] J. Liu, X. Chen, and X. Ji, Nat. Phys. **13**, 212 (2017).
[3] M. Schumann, J. Phys. G **46**, 103003 (2019).
[4] L. Bergström and P. Ullio, Nucl. Phys. **B504**, 27 (1997).
[5] O. Adriani *et al.* (PAMELA Collaboration), Nature (London) **458**, 607 (2009).
[6] M. Aguilar *et al.* (AMS Collaboration), Phys. Rep. **894**, 1 (2021).

[7] G. Ambrosi *et al.* (DAMPE Collaboration), Nature (London) **552**, 63 (2017).

[8] I. V. Moskalenko, A. W. Strong, S. G. Mashnik, and J. F. Ormes, Astrophys. J. **586**, 1050 (2003).

[9] D. Hooper, T. Linden, and P. Mertsch, J. Cosmol. Astropart. Phys. 03 (2015) 021.

[10] M.-Y. Cui, Q. Yuan, Y.-L. S. Tsai, and Y.-Z. Fan, Phys. Rev. Lett. **118**, 191101 (2017).

[11] A. Cuoco, M. Krämer, and M. Korsmeier, Phys. Rev. Lett. **118**, 191102 (2017).

[12] D. Hooper and L. Goodenough, Phys. Lett. B **697**, 412 (2011).

[13] B. Zhou, Y.-F. Liang, X. Huang, X. Li, Y.-Z. Fan, L. Feng, and J. Chang, Phys. Rev. D **91**, 123010 (2015).

[14] T. Daylan, D. P. Finkbeiner, D. Hooper, T. Linden, S. K. N. Portillo, N. L. Rodd, and T. R. Slatyer, Phys. Dark Universe **12**, 1 (2016).

[15] F. Calore, I. Cholis, and C. Weniger, J. Cosmol. Astropart. Phys. 03 (2015) 038.

[16] D. Hooper, P. Blasi, and P. D. Serpico, J. Cosmol. Astropart. Phys. 01 (2009) 025.

[17] P.-F. Yin, Z.-H. Yu, Q. Yuan, and X.-J. Bi, Phys. Rev. D **88**, 023001 (2013).

[18] Q. Yuan *et al.*, arXiv:1711.10989.

[19] M.-Y. Cui, X. Pan, Q. Yuan, Y.-Z. Fan, and H.-S. Zong, J. Cosmol. Astropart. Phys. 06 (2018) 024.

[20] M.-Y. Cui, W.-C. Huang, Y.-L. S. Tsai, and Q. Yuan, J. Cosmol. Astropart. Phys. 11 (2018) 039.

[21] I. Cholis, T. Linden, and D. Hooper, Phys. Rev. D **99**, 103026 (2019).

[22] S.-J. Lin, X.-J. Bi, J. Feng, P.-F. Yin, and Z.-H. Yu, Phys. Rev. D **96**, 123010 (2017).

[23] H.-B. Jin, Y.-L. Wu, and Y.-F. Zhou, Astrophys. J. **901**, 80 (2020).

[24] J. Heisig, M. Korsmeier, and M. W. Winkler, Phys. Rev. Res. **2**, 043017 (2020).

[25] A. Jueid, J. Kip, R. R. de Austri, and P. Skands, arXiv: 2202.11546.

[26] R. Bartels, S. Krishnamurthy, and C. Weniger, Phys. Rev. Lett. **116**, 051102 (2016).

[27] S. K. Lee, M. Lisanti, B. R. Safdi, T. R. Slatyer, and W. Xue, Phys. Rev. Lett. **116**, 051103 (2016).

[28] O. Macias, C. Gordon, R. M. Crocker, B. Coleman, D. Paterson, S. Horiuchi, and M. Pohl, Nat. Astron. **2**, 387 (2018).

[29] R. Bartels, E. Storm, C. Weniger, and F. Calore, Nat. Astron. **2**, 819 (2018).

[30] R. K. Leane and T. R. Slatyer, Phys. Rev. Lett. **123**, 241101 (2019).

[31] Y.-M. Zhong, S. D. McDermott, I. Cholis, and P. J. Fox, Phys. Rev. Lett. **124**, 231103 (2020).

[32] I. Cholis, Y.-M. Zhong, S. D. McDermott, and J. P. Surdutovich, Phys. Rev. D **105**, 103023 (2022).

[33] T. Aaltonen *et al.* (CDF Collaboration), Science **376**, 170 (2022).

[34] Y.-Z. Fan, T.-P. Tang, Y.-L. S. Tsai, and L. Wu, Phys. Rev. Lett. **129**, 091802 (2022).

[35] M. S. Potgieter, E. E. Vos, R. Munini, M. Boezio, and V. Di Felice, Astrophys. J. **810**, 141 (2015).

[36] X. Luo, M. S. Potgieter, V. Bindi, M. Zhang, and X. Feng, Astrophys. J. **878**, 6 (2019).

[37] M. Aguilar *et al.* (AMS Collaboration), Phys. Rev. Lett. **121**, 051101 (2018).

[38] X. Huang, T. Enßlin, and M. Selig, J. Cosmol. Astropart. Phys. 04 (2016) 030.

[39] L. J. Gleeson and W. I. Axford, Astrophys. J. **154**, 1011 (1968).

[40] I. Cholis, D. Hooper, and T. Linden, Phys. Rev. D **93**, 043016 (2016).

[41] L. Maccione, Phys. Rev. Lett. **110**, 081101 (2013).

[42] M. Zhang, Astrophys. J. **513**, 409 (1999).

[43] R. D. Strauss, M. S. Potgieter, I. Büsching, and A. Kopp, Astrophys. J. **735**, 83 (2011).

[44] E. N. Parker, Planet. Space Sci. **13**, 9 (1965).

[45] See Supplemental Material at http://link.aps.org/supplemental/10.1103/PhysRevLett.129.231101 for some supplemental analysis method, discussion, and figures.

[46] X. Luo, M. S. Potgieter, M. Zhang, and X. Feng, Astrophys. J. **839**, 53 (2017).

[47] E. N. Parker, Astrophys. J. **128**, 664 (1958).

[48] J. Kota and J. R. Jokipii, Astrophys. J. **265**, 573 (1983).

[49] J. R. Jokipii, E. H. Levy, and W. B. Hubbard, Astrophys. J. **213**, 861 (1977).

[50] R. A. Burger and M. S. Potgieter, Astrophys. J. **339**, 501 (1989).

[51] M. S. Potgieter, J. A. Le Roux, and R. A. Burger, J. Geophys. Res. **94**, 2323 (1989).

[52] A. C. Cummings, E. C. Stone, B. C. Heikkila, N. Lal, W. R. Webber, G. Jóhannesson, I. V. Moskalenko, E. Orlando, and T. A. Porter, Astrophys. J. **831**, 18 (2016).

[53] H. An, A. Kumamoto, R. Xiang, T. Inoue, K. Otsuka, S. Chiashi, C. Bichara, A. Loiseau, Y. Li, Y. Ikuhara, and S. Maruyama (DAMPE Collaboration), Sci. Adv. **5**, eaax3793 (2019).

[54] A. W. Strong and I. V. Moskalenko, Astrophys. J. **509**, 212 (1998), and https://galprop.stanford.edu/.

[55] Q. Yuan, C.-R. Zhu, X.-J. Bi, and D.-M. Wei, J. Cosmol. Astropart. Phys. 11 (2020) 027.

[56] C.-R. Zhu, Q. Yuan, and D.-M. Wei, Astrophys. J. **863**, 119 (2018).

[57] M. Aguilar, D. Aisa, B. Alpat, A. Alvino, G. Ambrosi, K. Andeen, L. Arruda, N. Attig, P. Azzarello, A. Bachlechner *et al.*, Phys. Rev. Lett. **114**, 171103 (2015).

[58] M. W. Winkler, J. Cosmol. Astropart. Phys. 02 (2017) 048.

[59] M. Kachelriess, I. V. Moskalenko, and S. S. Ostapchenko, Astrophys. J. **803**, 54 (2015).

[60] M. Aguilar *et al.* (AMS Collaboration), Phys. Rev. Lett. **117**, 091103 (2016).

[61] X. Sun, J. T. Hoeksema, Y. Liu, and J. Zhao, Astrophys. J. **798**, 114 (2015).

[62] S. E. S. Ferreira and M. S. Potgieter, Astrophys. J. **603**, 744 (2004).

[63] X. Song, X. Luo, M. S. Potgieter, X. Liu, and Z. Geng, Astrophys. J. Suppl. Ser. **257**, 48 (2021).

[64] C.-R. Zhu, Q. Yuan, and D.-M. Wei, Astropart. Phys. **124**, 102495 (2021).

[65] H. Zhao, Mon. Not. R. Astron. Soc. **278**, 488 (1996).

[66] J. D. Simon, Annu. Rev. Astron. Astrophys. **57**, 375 (2019).

[67] K. Hayashi, M. Ibe, S. Kobayashi, Y. Nakayama, and S. Shirai, Phys. Rev. D **103**, 023017 (2021).

[68] J. Alwall, R. Frederix, S. Frixione, V. Hirschi, F. Maltoni, O. Mattelaer, H. S. Shao, T. Stelzer, P. Torrielli, and M. Zaro, J. High Energy Phys. 07 (2014) 079.

[69] T. Sjöstrand, S. Ask, J. R. Christiansen, R. Corke, N. Desai, P. Ilten, S. Mrenna, S. Prestel, C. O. Rasmussen, and P. Z. Skands, Comput. Phys. Commun. **191**, 159 (2015).

[70] G. Steigman, B. Dasgupta, and J. F. Beacom, Phys. Rev. D **86**, 023506 (2012).

[71] M. Selig, V. Vacca, N. Oppermann, and T. A. Enßlin, Astron. Astrophys. **581**, A126 (2015).

[72] W. de Boer, I. Gebauer, A. Neumann, and P. L. Biermann, arXiv:1610.08926.

[73] W. de Boer, L. Bosse, I. Gebauer, A. Neumann, and P. L. Biermann, Phys. Rev. D **96**, 043012 (2017).

[74] K. M. Górski, E. Hivon, A. J. Banday, B. D. Wandelt, F. K. Hansen, M. Reinecke, and M. Bartelman, Astrophys. J. **622**, 759 (2005).

[75] M. Ackermann *et al.* (Fermi-LAT Collaboration), Astrophys. J. **750**, 3 (2012).

[76] M. Su, T. R. Slatyer, and D. P. Finkbeiner, Astrophys. J. **724**, 1044 (2010).

[77] S. Abdollahi *et al.* (Fermi-LAT Collaboration), Astrophys. J. Suppl. Ser. **247**, 33 (2020).

[78] S. Abdollahi *et al.* (Fermi-LAT Collabortion), Astrophys. J. Suppl. Ser. **260**, 53 (2022).

[79] C.-T. Lu, L. Wu, Y. Wu, and B. Zhu, Phys. Rev. D **106**, 035034 (2022).

[80] P. Athron, A. Fowlie, C.-T. Lu, L. Wu, Y. Wu, and B. Zhu, arXiv:2204.03996.

[81] R. Abbasi *et al.* (IceCube Collaboration), in *37th International Cosmic Ray Conference* (2021), arXiv:2107.11224.

[82] P. L. Biermann *et al.*, Adv. Space Res. **62**, 2773 (2018).

[83] P.-p. Zhang, B.-q. Qiao, Q. Yuan, S.-w. Cui, and Y.-q. Guo, Phys. Rev. D **105**, 023002 (2022).